SLAC-PUB-5749

August 1992

(A)

THE ANALYSIS OF TRANSVERSE BEAM TAIL DISTRIBUTIONS OF BUNCHES WITH NON-GAUSSIAN SHAPES*

M. S. Avilov# and J. T. Seeman

Stanford Linear Accelerator Center, Stanford, CA 94309 USA

ABSTRACT

The characterization of transverse particle distributions of bunches with non-Gaussian shapes is difficult due to a wide variety of possibilities [1]. Without knowing additional information one can fit a distribution using first-, second-, third-, and higher order moments [2]. These moments can then be used to describe beam shape changes along the accelerator, but with limited knowledge of the physics which caused the perturbed shape. However, when the cause of the non-Gaussian distribution is known, a more detailed description of the particle distribution can be constructed. In the Stanford Linear Collider (SLC) non-Gaussian distributions are produced by transverse wakefields in the 3000 m linac.

1 TRANSVERSE TAIL PARAMETERIZATION

The effects of transverse wakefields can be calculated given the transverse equation of motion of the particles in the bunch.

$$\frac{d^2}{ds^2} x(z,s) + k^2 (z,s)\, x(z,s) = \frac{r_e}{\gamma(z,s)} \int_z^{\infty} dz'\, h(z')W(z'-z)\, x(z',s), \tag{1}$$

where x is the transverse offset from the accelerator axis, s is the distance along the accelerator, z is the longitudinal distance along the bunch, k is the lattice strength, $\gamma = E/mc^2$, h is the longitudinal particle density, r_e is the classical radius of the electron, and W is the transverse wakefield which depends on the longitudinal separation of the particle generating the fields and the particle sensing the fields. The solution of this equation shows that oscillating leading particles drive trailing particles to larger amplitudes, generating non-Gaussian distributions [3]. A schematic view of such a transverse tail is shown in Figure 1, where the particle centroids move farther and farther off-axis near the end of the bunch. Also, with very strong wakefields or with special conditions used to reduce wakefield emittance growth (BNS damping), the transverse tails can spread out over circles in transverse phase space.

These longitudinal correlations of the displacement and angle of the various 'slices' along the bunch can be seen in Figure 2. The transverse particle distribution $\rho_i(x)$ of a longitudinal slice with label i which is on-axis is given by

$$\rho_i(x) = \frac{\exp(-x^2/2\,\varepsilon\,\beta_i)}{\sqrt{2\,\pi\,\varepsilon\,\beta_i}} \tag{2}$$

where $\sigma_x = \varepsilon\beta_i$. The overall distribution f representing the entire bunch is obtained by integrated over the bunch with the appropriate Δx_i indicating the offsets of the various slices.

$$f(x) = \sum_{i=1}^{n} \rho_i(x + \Delta x_i)\, h(z_i) \tag{3}$$

where n is the number of slices and h is (usually) a Gaussian with length σ_z. The offsets Δx_i can be described with an exponentially growing tail without curvature [1]. However, in this analysis a more complex form is used to include the curvature and varying growth factors. As indicated by many simulations, the place along the bunch where the tail starts to grow is about 0.5 σ_z in front of the bunch. That location is fixed in the calculation. Therefore, at the reference profile monitor the position and angle offsets are given by

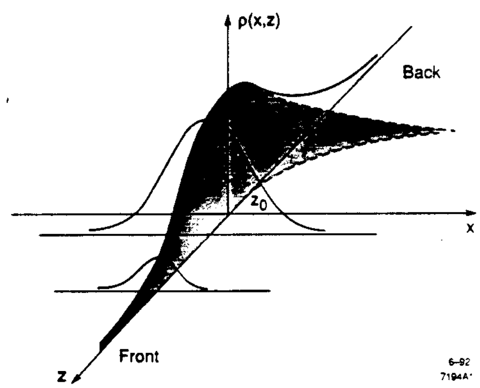

Figure 1 Schematic view of transverse offsets increasing from the front to the back of the bunch induced by transverse wakefields.

* Work supported by US Department of Energy contract AC03-76SF00515.

Visitor from the Institute of Nuclear Physics, Novosibirsk, Russia.

Presented at the XV International Conference on High Energy Accelerators, Hamburg, Germany, July 20-24, 1992.

$$\Delta x_1(z) = r\left(-\frac{z}{\sigma_z}+\frac{1}{2}\right)^d \cos\left(\frac{c\,z}{\sigma_z}+\phi_{\beta_0}\right)$$

$$\Delta x'_1(z) = \frac{r}{\beta}\left(-\frac{z}{\sigma_z}+\frac{1}{2}\right)^d \sin\left(\frac{c\,z}{\sigma_z}+\phi_{\beta_0}\right) - \frac{\alpha_1}{\beta_1}\Delta x_1(z) \qquad (4)$$

where r, c, d, and $\phi\beta$ are the fit parameters, $z < \sigma_z/2$, α_1, β_1, and γ_1 are the known lattice Twiss parameters at wire 1. These offsets can be translated to any wire downstream using the transport matrix elements R_{11} and R_{12} from wire 1 to wire i.

$$\Delta x_i = R_{11}\,\Delta x + R_{12}\,\Delta x'_1$$

$$\beta_i = R_{11}^2\,\beta_1 - 2\,R_{11}\,R_{12}\,\alpha_1 + R_{12}^2\,\gamma_1 \qquad (5)$$

$$\phi_\beta = \phi_{\beta_0} + \int \frac{ds}{\beta}$$

During the analysis of the data it is (reasonably) assumed that there are negligible additional wakefield effects internal to the measurement region. Thus, each particle in the bunch will oscillate with a free betatron oscillation through the measurement region as given by the quadrupole lattice and its initial conditions, taken here at the location of the most upstream wire scanner. Furthermore, in this analysis it is assumed that each slice of the beam is matched to the linac lattice because filamentation has forced a matched beam.

Transverse profiles in the SLC are measured using moving wire scanners[4]. Four scanners are spaced over about 120 to 240 degrees of betatron phase advance. Multiple measurements on each wire are used to improve accuracy. The beam sizes vary from 80 to 200 μm. The wire diameters are 45 to 70 μm. The resolution of a width measurement is 3 - 5 μm.

An application program simultaneously fits the profile data from four scanners to the above model using 17 fit variables:

$X_1,\ldots,X_4$	= centers of the bunches on wires 1,...,4.
$a_1,\ldots,a_4$	= amplitudes of the beam cores on wires 1,...,4.
$b_1,\ldots,b_4$	= flat background levels on wires 1,...4,
ε_0	= beam core emittance.
r	= phase space tail amplitude.
c	= phase space curvature of tail in phase space.
d	= offset exponent of tail slices from the head.
$\phi\beta$	= tail betatron phase on wire 1.

The bunch is divided into 20 longitudinal slices, each characterized by different displacements. The longitudinal lengths of the slices are varied to place more slices at the end of the bunch where the offsets are the largest and improved resolution is needed. The displacements of the slices are transported between the wire scanners using the lattice betatron phase advances, which are 0, 22.5, 90, and 112.5 degrees for the data shown below. The fit is non-linear due to the tail parameters and is done using a chi-squared value function and a non-linear minimization routine (UMCGG [5]) requiring about 15 seconds of CPU time. Let the measured transverse distributions be given by $Y_i(x)$, then the value function for the combined four wires which is to be minimized is given by

$$F = \sum_{i=1}^{4}\sum_{j=1}^{m} \left(b_i + a_i\, f_i(x_j) - Y_i(x_j)^2 \right) \qquad (6)$$

where m is the number of samples for wire i. The initial parameters for the non-linear fit are taken from the four Gaussian fits to the distributions assuming no tails.

The ratio of the emittance of the transverse tail of the beam to that of the beam core can be calculated from the reconstructed phase space locations of the slices. The effective emittance of the entire bunch is calculated similarly to Ref. [6] except that the position of the head of the bunch is defined to be on-axis. The centering of the two beams at the SLC interaction point using beam-beam deflections aligns the cores of the bunches.

$$\varepsilon_{eff}^2 = \langle xx\rangle\langle x'x'\rangle - \langle xx'\rangle^2 \qquad (7)$$

where

$$\langle xx\rangle = \sum_{k=1}^{n} \frac{Q_k}{Q}\left(\langle xx\rangle_k + \Delta x_k^2 \right), \qquad (8)$$

Q is the total charge of the bunch, Q_k is the charge of the k-th slice, $\langle xx\rangle_k$ is the square of the transverse size of the k-th slice, and Δx_k is the center of the k-th slice. Analogous expressions for $\langle xx'\rangle$ and $\langle x'x'\rangle$ are used. A ratio of the tail emittance to core emittance $T = (\varepsilon_{eff} - \varepsilon_0)/\varepsilon_0$ is a convenient parameter to describe the tail effects on the luminosity.

2 EXAMPLES OF SLC DATA

The fit parameters are written in a data file and appropriate displays made. For example, the resulting fits are superimposed on the data from the four wires for monitoring

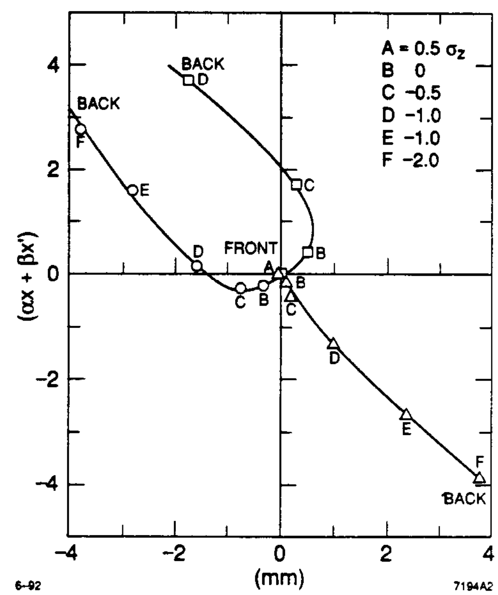

Figure 2 Three examples of simulated bunch slice offsets under different conditions showing curvature in phase space which increases at various rates from the front to the back of the bunch.

fit accuracy. Two examples of these simultaneous fits are shown here for data taken at 47 GeV with 2.7 x 10^{10} electrons. In Figure 3, the data show the near exponential growth of the tail without curvature in phase space. In Figure 4 different data indicate significant phase space curvature of the tail. The reconstructed locations of the longitudinal slices can be shown in phase space to indicate the direction and extent of the tail as represented at the first wire scanner, see Figures 3 and 4. The area of each ellipse is proportional to the charge in that slice. These displays suggest the corrections needed to the beam trajectories to cancel these emittance enlargement errors [7]. For the data in Figures 3 and 4, the T parameter is about 1.0.

3 REFERENCES

[1] J. T. Seeman, *et al.*, *Proc. of IEEE USPAC*, San Francisco, p. 1734 (1991).

[2] W. Spence, private communication (1992).

[3] J. Seeman, *Annu. Rev. of Nucl. Part. Sci.*, p. 389 (1991).

[4] M. Ross, *et al.*, *Proc. of IEEE USPAC*, San Francisco, 91CH3038-7, p. 1201 (1991).

[5] Digital Equipment Corporation, Massachusetts, USA.

[6] K. Bane, SLAC-PUB-4169, SLAC (1986).

[7] J. Seeman, et al, *Proc. of HEACC*, Hamburg (1992).

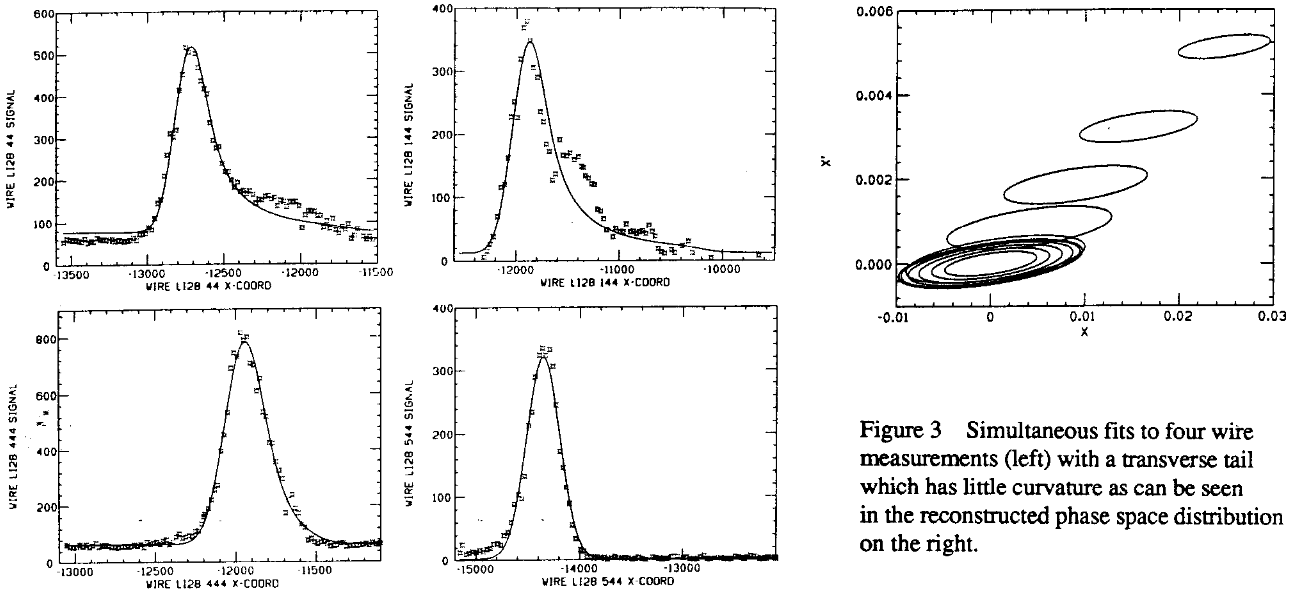

Figure 3 Simultaneous fits to four wire measurements (left) with a transverse tail which has little curvature as can be seen in the reconstructed phase space distribution on the right.

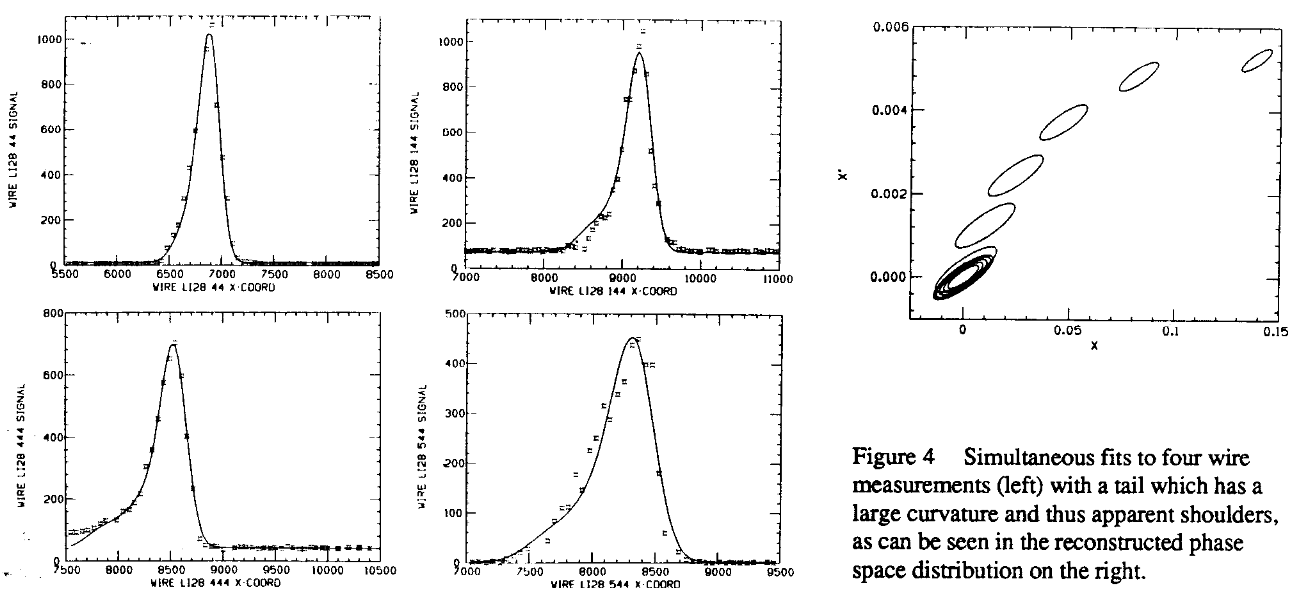

Figure 4 Simultaneous fits to four wire measurements (left) with a tail which has a large curvature and thus apparent shoulders, as can be seen in the reconstructed phase space distribution on the right.